EXAMPLE 7-5

During the infiltration event of Example 6-7 a total of 81.4 mm infiltrated. Following this, stage-1 evaporation lasted for $t_1 = 3$ days and occurred at an average rate of $\overline{E}_1 = 10 \text{ mm day}^{-1}$. Compute the stage-2 evaporation rate over the next 10 days in which no rain fell.

Solution From Equation (7-43), the stage-1 evaporation is

$$F_1 = 10 \text{ mm day}^{-1} \cdot 3 \text{ day} = 30 \text{ mm}.$$

For stage 2, Equation (7-44) gives the cumulative evaporation:

$$F_{soil}(t) = 30\,\text{mm} \cdot \left[1 + 0.811 \cdot \ln\left(\frac{t}{3\,\text{day}}\right)\right];$$

and Equation (7-45) gives the evaporation rate:

$$E_2(t) = 0.811 \cdot 10 \text{ mm day}^{-1} \cdot \frac{3 \text{ day}}{t} = \frac{24.3 \text{ mm}}{t}.$$

The results are tabulated as follows:

t (day)	3.0	3.5	4.0	4.5	5.0	5.5	6.0
$E_2(t)$ (mm day^{-1})	8.11	6.95	6.08	5.40	4.86	4.42	4.05
$F_{soil}(t)$ (mm)	30.0	33.8	37.0	39.9	42.4	44.7	46.9

t (day)	6.5	7.0	7.5	8.0	8.5	9.0	9.5	10.0
$E_2(t)$ (mm day^{-1})	3.74	3.47	3.24	3.04	2.86	2.70	2.56	2.43
$F_{soil}(t)$ (mm)	48.8	50.6	52.3	53.9	55.3	56.7	58.0	59.3

7.5 TRANSPIRATION

7.5.1 The Transpiration Process

Transpiration is the evaporation of water from the vascular system of plants into the atmosphere. The entire process (Figure 7-9) involves **absorption** of soil water by plant roots; **translocation** in liquid form through the vascular system of the roots, stem, and branches to the leaves; and translocation through the vascular system of the leaf to the walls of tiny **stomatal cavities,** where evaporation takes place. The water vapor in these cavities then moves into the ambient air through openings in the leaf surface called **stomata.**

Plants live by absorbing carbon dioxide (CO_2) from the air to make carbohydrates, and that gas can enter the plant only when dissolved in water. The essential function of the stomatal cavities is to provide a place where CO_2 dissolution can occur and enter plant tissue; the evaporation of water is an unavoidable concomitant of that process. However, transpiration also performs the essential functions of maintaining the turgor of plant cells and delivering mineral nutrients from the soil to growing tissue.

Air in stomatal cavities is saturated at the temperature of the leaf, and water moves from the cavities into the air due to a vapor-pressure difference, just as in open-water evaporation. The major difference between transpiration and open-water evaporation is that plants can exert some physiological control over the size of the stomatal openings, and hence the ease of vapor movement, by the action of **guard cells** (Figure 7-10). The major factors affecting the opening and closing of guard cells are (1) light (most plants open stomata during the day and close them at night), (2) humidity (stomatal openings tend to decrease as humidity decreases below its saturation value), and (3) the water content of the leaf cells (if daytime water contents become too low, stomata tend to close).[7]

It is important to emphasize that transpiration is a physical, not a metabolic, process: Water in the **transpiration stream** is pulled through the plant by potential-energy gradients that originate with the movement of water vapor into the air through the stomata in response to a vapor-pressure difference. When vapor exits through the stomata, water evaporates from the walls of the stomatal cavity to replace the loss; this loss of liquid water causes a potential-energy decrease that induces the movement of replacement water up through the vascular system; this movement ultimately produces a water-

---

[7] Several other factors are known to affect the opening and closing of stomata, including wind, CO_2 levels, temperature, and certain chemicals. A mathematical representation of the effects of the factors most important in hydrological modeling is given later.

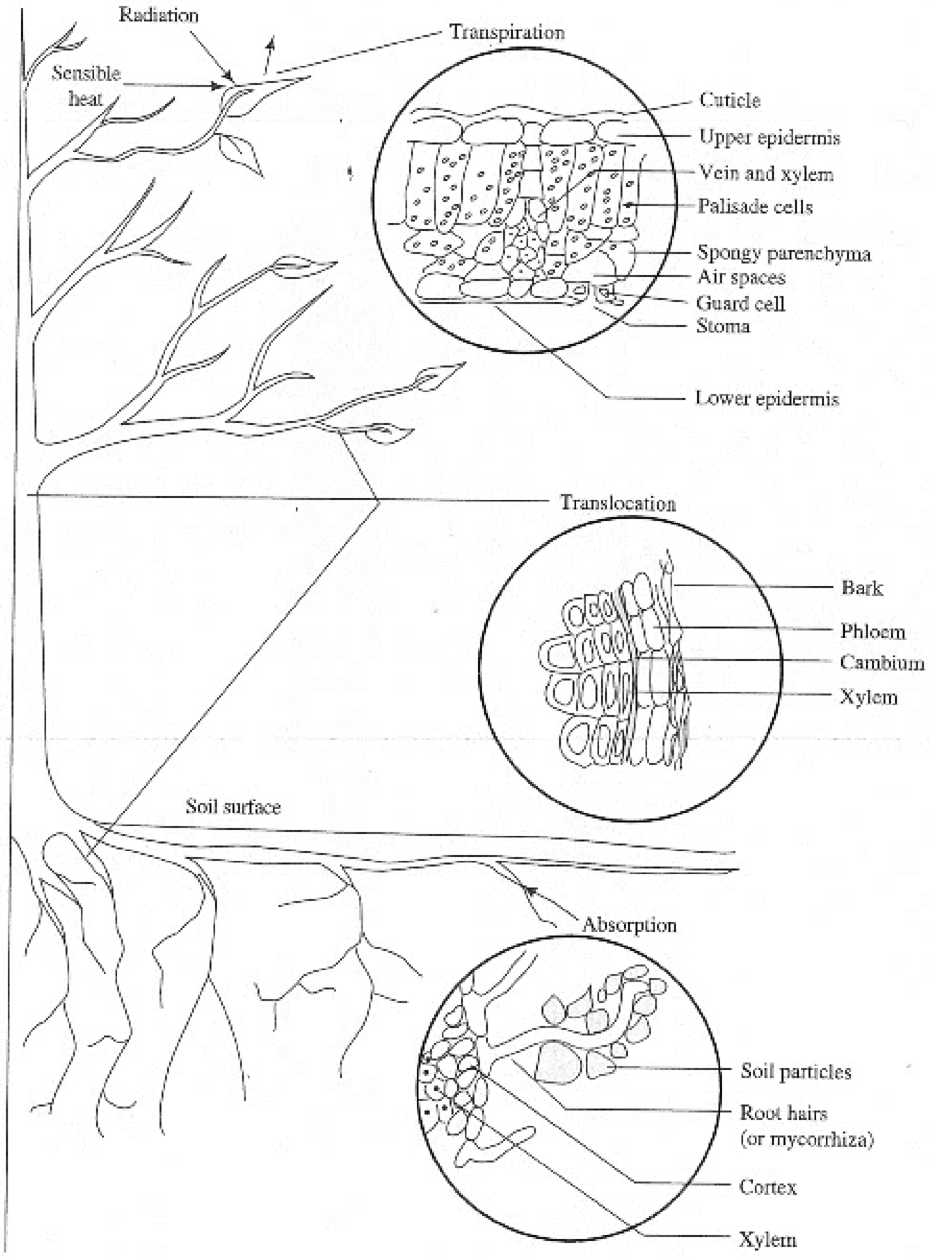

FIGURE 7-9
Diagram of the transpiration process and enlarged views of plant cellular structure where absorption, translocation, and transpiration occur. From Hewlett (1992).

content gradient between the root and the soil; and this gradient induces movement of soil water into the root. Absorption at the root surface decreases soil-water content in the adjacent soil, inducing some flow of water toward the root following Darcy's Law [Equation (6-10)]. However, roots come into contact with soil water mostly by growing toward the water: During the growing season roots typically grow several tens of millimeters per day (Raven et al. 1976).

The great cohesive strength of water due to its intermolecular hydrogen bonds (see Section B.1.1) maintains the integrity of the transpiration stream to heights of the tallest trees.

7.5.2 Modeling Transpiration

Since transpiration is essentially the same physical process as open-water evaporation, it can be represented by a mass-transfer equation of the form of

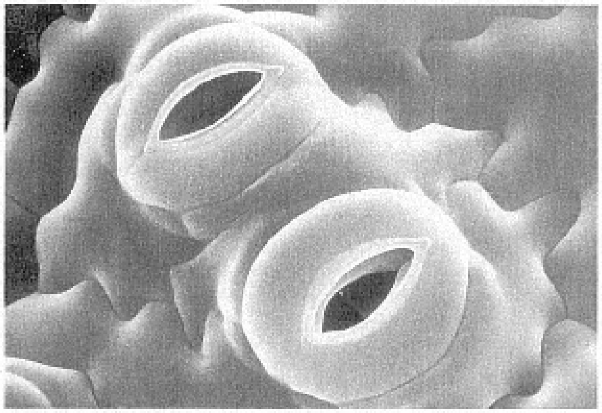

FIGURE 7-10
Photomicrograph of leaf surface showing stomata and the crescent-shaped guard cells that regulate their openings.
Dr. Jeremy Burgess/Science Photo Laboratory.

Equation (7-1). In order to develop an equivalent relation for transpiration, it is convenient first to recast the mass-transfer relation for evaporation using the concept of atmospheric conductance. This allows us to use some electric-circuit analogies for "scaling up" from a leaf to an entire vegetated surface.

Atmospheric Conductance

We can represent the process of evaporation from open water by combining Equations (7-1) and (7-2) and defining an "atmospheric constant", K_{at}, as

$$K_{at} \equiv \frac{0.622 \cdot \rho_a}{P \cdot \rho_w}, \qquad \textbf{(7-46)}$$

so that

$$E = K_{at} \cdot \left\{ \frac{D_V \cdot v_a}{D_M \cdot 6.25 \cdot \left[\ln\left(\frac{z_m - z_d}{z_0} \right) \right]^2} \right\} \cdot (e_s - e_a), \qquad \textbf{(7-47)}$$

where D_V and D_M are the diffusivities of water vapor and momentum, respectively [equations (D-25) and (D-30).

The term in braces in Equation (7-47) represents the efficiency of the turbulent eddies in the lower atmosphere in transporting water vapor from the surface to the ambient air. This can also be viewed as an **atmospheric conductance** for water vapor, C_{at}, so that the mass-transfer equation for evaporation can be written as

$$\underset{\substack{\text{evaporation}\\ \text{rate}}}{E} = \underset{\substack{\text{atmospheric}\\ \text{constant}}}{K_{at}} \cdot \underset{\substack{\text{atmospheric}\\ \text{conductance}}}{C_{at}} \cdot \underset{\substack{\text{driving}\\ \text{gradient}}}{(e_s - e_a)}. \qquad \textbf{(7-48)}$$

If D_V is assumed identical to D_M,[8] C_{at} is given explicitly as

$$C_{at} \equiv \frac{v_a}{6.25 \cdot \left[\ln\left(\frac{z_m - z_d}{z_0} \right) \right]^2} \qquad \textbf{(7-49)}$$

and has the dimensions $[\mathrm{L\,T^{-1}}]$.[9]

The zero-plane displacement, z_d, and roughness height, z_0, can be approximately related to the height of vegetation, z_{veg}, as

$$z_d = 0.7 \cdot z_{veg} \qquad \textbf{(7-50)}$$

and

$$z_0 = 0.1 \cdot z_{veg}. \qquad \textbf{(7-51)}$$

If it is assumed that z_m is 2 m above the top of the vegetation, Equations (7-49)–(7-51) can be used to generate a relation between atmospheric conductance and wind speed for various values of z_{veg}, as shown in Figure 7-11. Typical values of z_{veg} for various land-cover types are given in Table 7-5.

Since evaporation from an open-water surface is a "one-step" process in which water molecules pass directly from the liquid surface into the atmosphere, it can be conceptually represented by the electric-circuit analogy shown in Figure 7-12a. In this analogy a current (water vapor) moves in response to a voltage (vapor-pressure difference) across a resistance (inverse of the atmospheric conductivity).

Leaf Conductance

Transpiration is a "two-step" process, in which water molecules pass (1) from the stomatal cavity to the leaf surface, and (2) from the leaf surface into the

---

[8] This assumption is justified for short vegetation, but becomes less so for forests because z_0 and z_d for water-vapor transfer increasingly differ from their values for momentum transfer as the surface gets rougher (C.A. Federer, pers. comm.). In the interests of simplicity, we assume $D_V = D_M$ in the developments herein.

[9] Many authors use **atmospheric resistance,** which is the inverse of atmospheric conductance.

FIGURE 7-11

Relation between atmospheric conductance, C_{at}, and wind speed, v_a, for vegetation of various heights, z_{veg}. Relation for typical water surface is also shown. It is assumed that v_a is measured 2 m above the canopy and that atmospheric stability is near neutral.

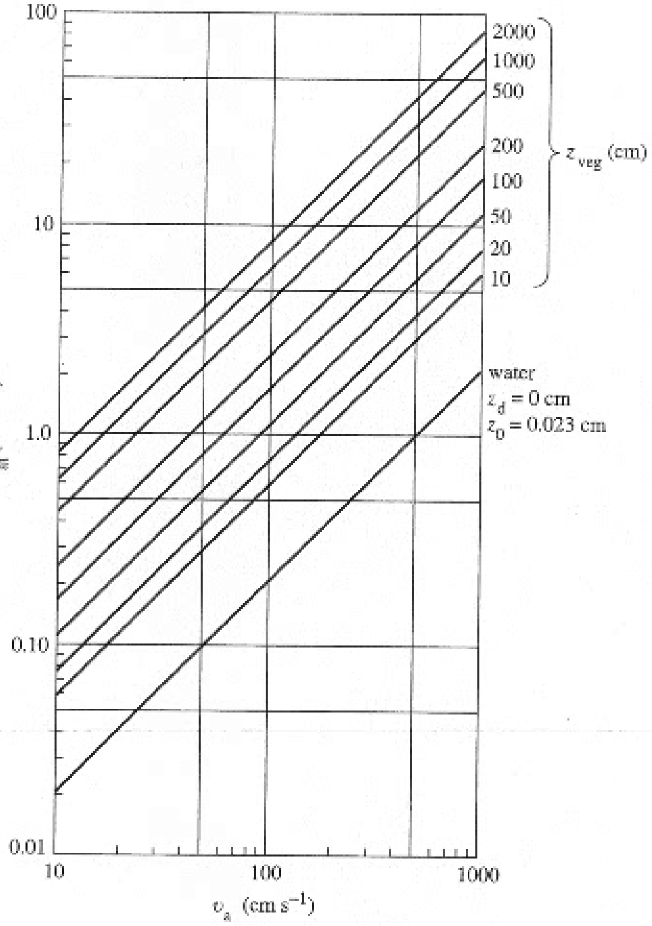

TABLE 7-5

Typical values of maximum leaf conductance (C^*_{leaf}), leaf-area index (*LAI*), albedo (*a*), and height (z_{veg}) for principal land-cover types.

Land Cover	C^*_{leaf} (mm s^{-1})	*LAI*	*a*	z_{veg} (m)
Conifer forest	5.3	6.0	0.14	25.0
Broadleaf forest	5.3	6.0	0.18	25.0
Savannah/shrub	5.3	3.0	0.18	8.0
Grassland	8.0	3.0	0.20	0.5
Tundra/nonforest wetland	6.6	4.0	0.20	0.3
Desert	5.0	1.0	0.26	0.1
Typical crop	11.0	3.0	0.22	0.3

Data from Federer et al. (1996).

atmosphere. Continuing the electric-circuit analogy, the same driving force in this case operates across two resistances (inverse conductances) linked in series: leaf and atmospheric (Figure 7-12b).

Leaf conductance is determined by the number of stomata per unit area and the size of the stomatal openings. Stomatal densities range from 10,000 to 100,000 stomata per square centimeter of leaf surface, depending on species (Hewlett 1982). Table 7-5 lists leaf conductances at maximum stomatal opening for various land-cover types. As noted earlier, plants control the size of the stomatal openings, and hence leaf conductance, by the response of the guard cells. These cells have been found to respond to (1) light intensity, (2) ambient CO_2 concentration, (3) leaf-air vapor-pressure difference, (4) leaf temperature, and (5) leaf water content (Stewart 1989). We first examine how these factors affect leaf conductance, and then incorporate them in a model for the transpiration from a vegetative canopy.

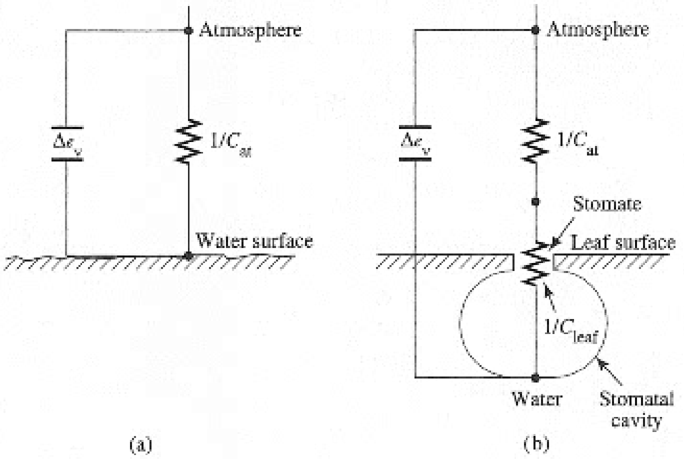

FIGURE 7-12
Conceptualization of (a) open-water evaporation and (b) evapotranspiration in terms of atmospheric resistance ($1/C_{at}$) and leaf resistance ($1/C_{leaf}$). Δe_v is the driving vapor-pressure difference between the evaporating surface and the atmosphere.

Stewart (1988) developed and tested a model for estimating hourly evapotranspiration that incorporates four of the five factors that determine leaf conductance—the effect of CO_2 concentration was not included because it usually varies little with time.[10] As shown in Table 7-6, he substituted more commonly measured hydrologic variables for some of the controlling factors—in particular, soil-water deficit was used as a proxy for leaf-water content. His model has the general form

$$C_{\text{leaf}} = C^{*}_{\text{leaf}} \cdot f_k(K_{\text{in}}) \cdot f_\rho(\Delta\rho_v) \cdot f_T(T_a) \cdot f_\theta(\Delta\theta), \qquad \textbf{(7-52)}$$

where C^{*}_{leaf} is the maximum value of leaf conductance (i.e., values from Table 7-5), K_{in} is incident short-wave radiation flux, $\Delta\rho_v$ is the humidity deficit [the difference between the saturated and actual absolute humidity of the air, calculated from vapor pressures and temperature via Equation (D-8)], T_a is air temperature, and $\Delta\theta$ is the soil-moisture deficit (the difference between the field capacity and the actual water content of the root zone).

The *f*s in Equation (7-52) represent the effects of each environmental factor on relative leaf conductance; they are non-linear functions that vary from 0 to 1 as shown in Figure 7-13. While the constants in these functions have been derived from studies at only one site (a pine forest in southeast England), controlled studies indicate that their form is quite general (Jarvis 1976). An abbreviated form of the model incorporating only $f_K(K_{\text{in}})$ and $f_\rho(\Delta\rho_v)$ (but with different constants, determined by calibration at the site) successfully modeled transpiration from prairie grasses in Kansas (Stewart and Gay 1989).

Canopy Conductance

A vegetated surface like a grass, crop, or forest canopy can be thought of as a large number of leaf conductances in parallel. Again from the laws of electric circuits, the total conductance of a number of conductances in parallel equals the sum of the individual conductances. Thus it is possible to represent a reasonably uniform vegetated surface as a single "big leaf" whose total conductance to water vapor is proportional to the sum of the conductances of millions of individual leaves. The relative size of this big leaf is reflected in the **leaf-area index**, *LAI*, defined as

$$LAI \equiv \frac{\text{total area of leaf surface above ground area } A}{A}. \qquad \textbf{(7-53)}$$

Canopy conductance is then given by

$$C_{\text{can}} = f_s \cdot LAI \cdot C_{\text{leaf}}, \qquad \textbf{(7-54)}$$

where f_s is a **shelter factor** that accounts for the fact that some leaves are sheltered from the sun and wind and thus transpire at lower rates. Values of f_s range from 0.5 to 1, and decrease with increasing *LAI* (Carlson 1991); a value of $f_s = 0.5$ is probably a good estimate for a completely vegetated area (Allen et al. 1989).

---

[10] However, a long-term decrease in leaf conductance is a possible response of plants to the anthropogenic increase in atmospheric CO_2 concentration, as discussed in Section 3.2.9 (Rosenberg et al. 1989).

TABLE 7-6
Stewart's (1988) model of leaf conductance as a function of environmental factors. Functional relations are plotted in Figure 7-13.

Factor Controlling Stomatal Opening	Quantity Representing Controlling Factor in Model	Functional Relation
light	incident solar radiation (MJ m^{-2} day^{-1})	$f_K(K_{in}) = \dfrac{12.78 \cdot K_{in}}{11.57 \cdot K_{in} + 104.4}$ $0 \leq K_{in} \leq 86.5$ MJ m^{-2} day^{-1}
CO_2 concentration	(not included)	(none)
vapor-pressure deficit	absolute-humidity deficit, $\Delta\rho_v$ (kg m^{-3})	$f_\rho(\Delta\rho_v) = 1 - 66.6 \cdot \Delta\rho_v$, $0 \leq \Delta\rho_v \leq 0.01152$ kg m^{-3}; $f_\rho(\Delta\rho_v) = 0.233$, 0.01152 kg $m^{-3} \leq \Delta\rho_v$
leaf temperature	air temperature, T_a (°C)	$f_T(T_a) = \dfrac{T_a \cdot (40 - T_a)^{1.18}}{691}$ $0 \leq T_a \leq 40$°C
leaf water content	soil-moisture deficit, $\Delta\theta$ (cm)	$f_\theta(\Delta\theta) = 1 - 0.00119 \cdot \exp(0.81 \cdot \Delta\theta)$ $0 \leq \Delta\theta \leq 8.4$ cm

Leaf-area indices for various types of plant communities are given in Table 7-5. For deciduous forests, leaf area changes through the growing season, rising from near 0 to a maximum and back; Figure 7-14 shows the seasonal variation of LAI used in modeling transpiration for three types of forests.

The Penman-Monteith Model

Making use of Equation (7-1) and the definitions of γ [Equation (7-13)], K_{at} [Equation (7-46)], and C_{at} [Equation (7-49)], the Penman (combination) model for evaporation from a free-water surface [Equation (7-33)] can be written in terms of atmospheric conductance as

$$E = \frac{\Delta \cdot (K + L) + \rho_a \cdot c_a \cdot C_{at} \cdot e_a^* \cdot (1 - W_a)}{\rho_w \cdot \lambda_v \cdot (\Delta + \gamma)}. \tag{7-55}$$

Recall that the derivation of this equation assumes no water-advected energy, no ground-heat conduction, and no heat-storage effects.

Monteith (1965) showed how the Penman equation can be modified to represent the evapotranspiration rate, ET, from a vegetated surface by incorporating canopy conductance:

$$ET = \frac{\Delta \cdot (K + L) + \rho_a \cdot c_a \cdot C_{at} \cdot e_a^* \cdot (1 - W_a)}{\rho_w \cdot \lambda_v \cdot [\Delta + \gamma \cdot (1 + C_{at}/C_{can})]}. \tag{7-56}$$

This relationship has become known as the **Penman-Monteith Equation.** The assumptions of no water-advected energy and no heat-storage effects, which are generally not valid for natural water bodies, are usually reasonable when considering a vegetated surface. (The term for ground-heat conduction can be included with $K + L$ if it is significant.) Note that Equation (7-56) reduces to Equation (7-55) when $C_{can} \rightarrow \infty$.

The Penman-Monteith Equation has been successfully tested in many environments [see, for example, Calder (1977), (1978); Berkowicz and Prahm (1982); Lindroth (1985); Dolman et al. (1988); Stewart (1988); Stewart and Gay (1989); Allen et al. (1989); Lemeur and Zhang (1990)] and has become the most widely used approach to estimating evapotranspiration from land surfaces. The following example shows how it can be applied.

EXAMPLE 7-6

Compare the evapotranspiration rate from the canopy for soil-moisture deficits of 0 cm and 7.0 cm at the pine forest at Thetford, England, in August. The following conditions apply (Stewart 1988): $z_{veg} = 16.5$ m; $LAI = 2.8$; $f_s = 0.5$; $C^*_{leaf} = 2.3$ mm s^{-1}; $P = 101.3$ kPa; $K_{in} = 25.1$ MJ m^{-2} s^{-1}; $a = 0.18$; $L = -4.99$ MJ m^{-2} s^{-1}; $T_a = 19.2$ °C; $W_a = 0.54$; $v_a = 3.00$ m s^{-1}.

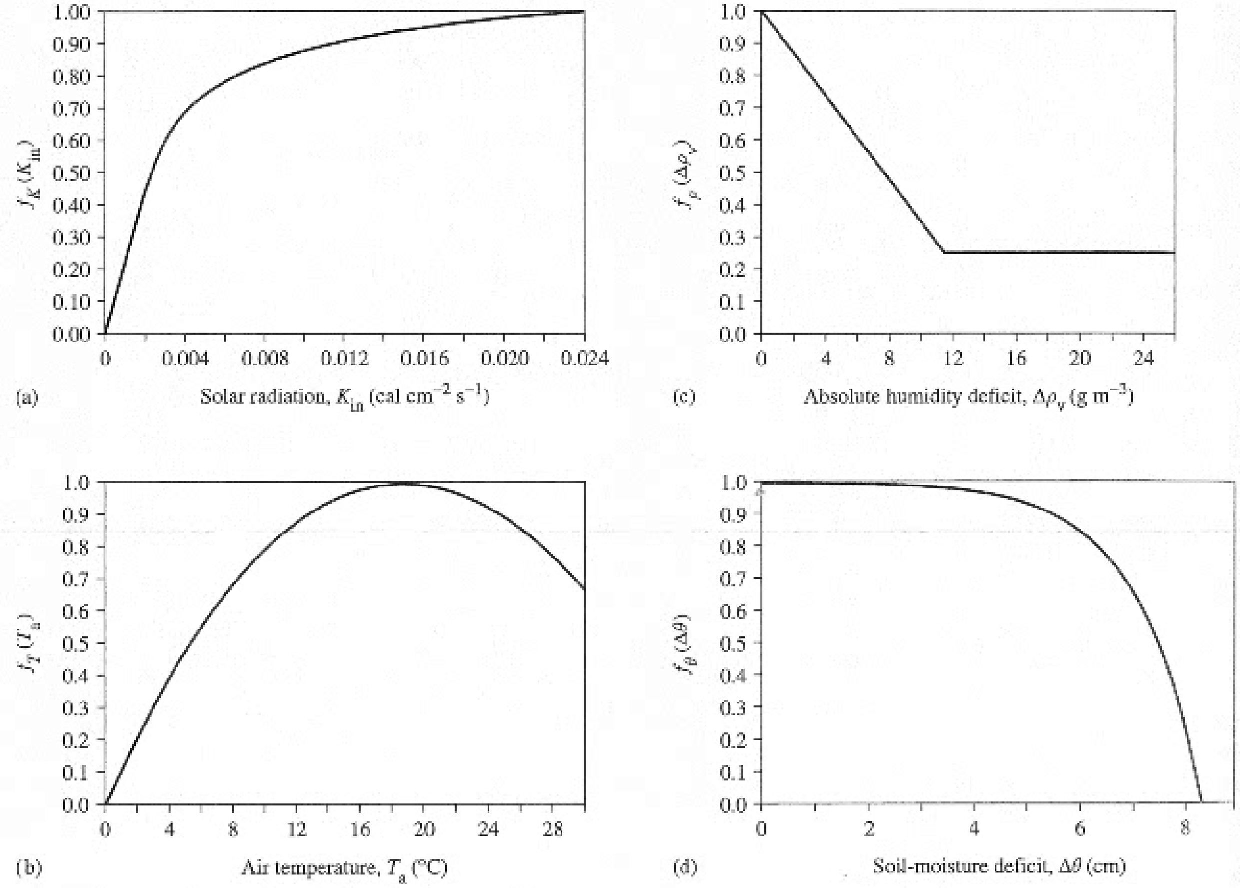

FIGURE 7-13

Effects of (a) solar radiation, K_{in}; (b) air temperature, T_a; (c) vapor-pressure deficit, $\Delta\rho_v$; and (d) soil-moisture deficit, $\Delta\theta$, on relative leaf conductances. (See Table 7-6.) After Stewart (1988).

(The values of z_{veg}, *LAI*, C^*_{leaf}, and *a* were determined for this site, so are used in preference to values from Table 7-5.)

Solution Applying equations given in this chapter we have

Quantity	Equation	Value
λ_v	(7-8)	2.45 MJ kg^{-1}
e^*_a	(7-4)	2.23 kPa
Δ	(7-6)	0.139 kPa K^{-1}
γ	(7-13)	0.0666 kPa K^{-1}
C_{at}	(7-49)–(7-51)	0.232 m s^{-1}

The vapor-pressure deficit, Δe_a, is found as

$$\Delta e_a = e^*_a \cdot (1 - W_a) = 2.23 \cdot (1 - 0.54)$$
$$= 1.03 \text{ kPa};$$

using this value in Equation (D-8c) yields $\Delta\rho_v = 7.62 \times 10^{-3}$ kg m^{-3}. Now we can compute the values of the *f*-functions given in Table 7-6:

Quantity	Value
$f_K(K_{in})$	0.812
$f_\rho(\Delta\rho_v)$	0.493
$f_T(T_a)$	0.998
$f_\theta(\Delta\theta = 0 \text{ cm})$	1.000
$f_\theta(\Delta\theta = 7 \text{ cm})$	0.655

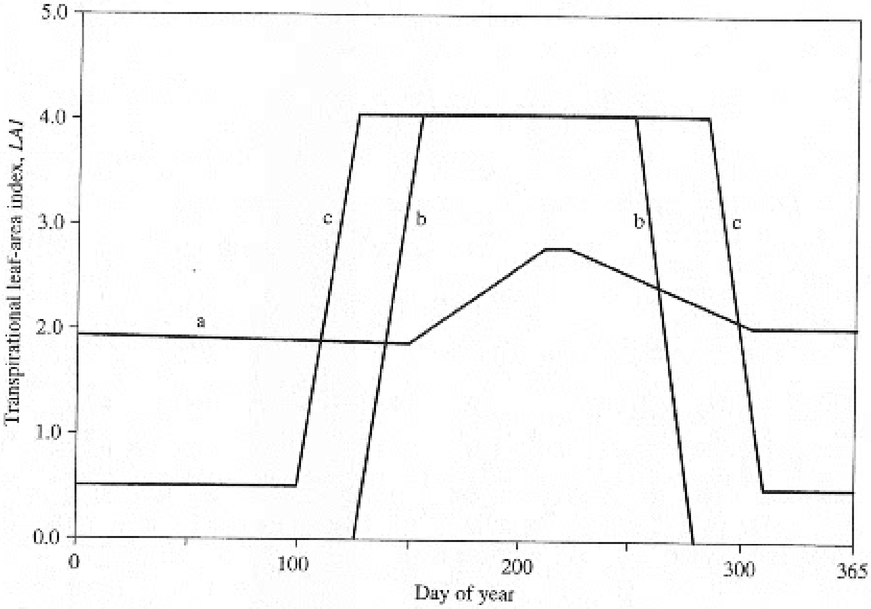

FIGURE 7-14
Annual variability of transpirational leaf-area index, *LAI*, in (a) a pine forest in southeast England (Stewart 1988); (b) a hardwood forest in New Hampshire; and (c) a hardwood forest in North Carolina [both from Federer and Lash (1978)].

From the above *f*-values we calculate the following conductances:

Quantity	Equation	Value (mm s^{-1})
C_{leaf} ($\Delta\theta = 0$ cm)	(7-52)	0.918
C_{leaf} ($\Delta\theta = 7$ cm)	(7-52)	0.602
C_{can} ($\Delta\theta = 0$ cm)	(7-54)	1.29
C_{can} ($\Delta\theta = 7$ cm)	(7-54)	0.843

Substituting the appropriate values from above into Equation (7-56) yields $ET = 1.04 \times 10^{-5}$ mm s^{-1} (= 0.9 mm day^{-1}) when $\Delta\theta = 0$ cm and $ET = 6.88 \times 10^{-6}$ mm s^{-1} (= 0.6 mm day^{-1}) when $\Delta\theta = 7$ cm.

We will consider the Penman-Monteith Equation further in discussing methods of estimating areal evapotranspiration (Section 7.8).

7.6 INTERCEPTION AND INTERCEPTION LOSS

Interception is the process by which precipitation falls on vegetative surfaces (the **canopy**), where it is subject to evaporation. As we will see, the intercepted water that is evaporated (**interception loss**) is a significant fraction of total evapotranspiration in most regions.

Interception loss depends strongly on (1) vegetation type and stage of development, which should be well characterized by leaf-area index; and (2) the intensity, duration, frequency, and form of precipitation. Vegetation type is commonly altered by human activities (e.g., deforestation), and there is concern that aspects of precipitation climatology may be altered by climate change (Waggoner 1989). A sound physical basis for understanding the interception process is essential in order to sort out and predict how these changes will affect the hydrologic cycle locally and globally. In particular, the question of whether interception loss is an addition to, as opposed to a replacement for, transpiration loss is important in evaluating the effects of vegetation changes on regional water balances.

Contact of precipitation with vegetation can significantly alter the chemical composition of water reaching the ground; thus interception can also influence weathering processes and water quality.

Under some weather conditions, vegetation can "comb" water from clouds and fog and thereby add water input to a region. This phenomenon is sometimes called "positive interception;" it is briefly discussed as "occult precipitation" in Section 4.2.2. Snow interception is treated in Section 5.3.2.

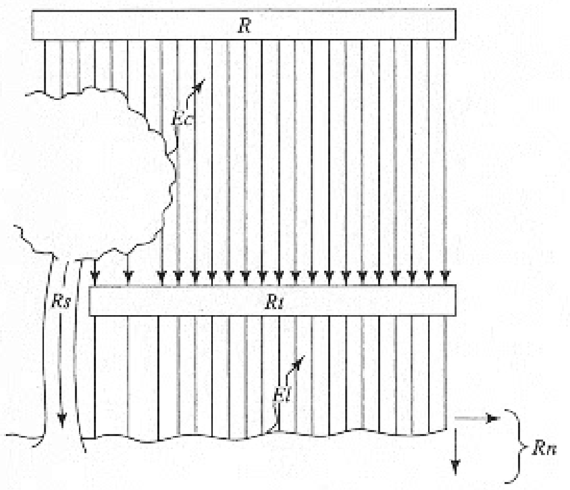

FIGURE 7-15
Definitions of terms used in describing the interception process. R = gross rainfall; Ec = canopy interception loss; Rt = throughfall; Rs = stemflow; El = litter interception loss; Rn = net rainfall.

7.6.1 Definitions

Figure 7-15 illustrates the following definitions used in describing and measuring interception:

Gross rainfall, R, is the rainfall measured above the vegetative canopy or in the open.

Throughfall, Rt, is rainfall that reaches the ground surface directly through spaces in the canopy and by dripping from the canopy.

Stemflow, Rs, is water that reaches the ground surface by running down trunks and stems.

Canopy interception loss, Ec, is water that evaporates from the canopy.

Litter interception loss, El, is water that evaporates from the ground surface (usually including near-ground plants and leaf litter).

Total interception loss, Ei, is the sum of canopy and litter interception losses.

Net rainfall, Rn, is the gross rainfall minus the total interception loss.

These definitions are applied over a representative area of the plant community of interest, so they take into account the typical spacing between plants. If the symbols given represent volumes of water during a given time period and have dimensions [L], we have

$$Rn = R - Ei, \tag{7-57}$$

$$Ei = Ec + El, \tag{7-58}$$

$$R = Rt + Rs + Ec, \tag{7-59}$$

and

$$Rn = Rt + Rs - El. \tag{7-60}$$

7.6.2 Measurement

As with other components of evapotranspiration, interception loss cannot be measured directly. The most common approach to determining the amounts of canopy interception loss in various plant communities is to measure gross rainfall, throughfall, and stemflow, and solve Equation (7-59) for Ec. However, this is not a simple procedure because of (1) the difficulties in accurately measuring rainfall, particularly at low rainfall intensities when interception losses are relatively large (see Section 4.2.2); (2) the large spatial variability of throughfall; and (3) the difficulty and expense of measuring stemflow.

Helvey and Patric (1965a) reviewed criteria for measuring interception quantities and concluded that averaging the catches in 20 rain gages spaced randomly over a representative portion of the community should give acceptable estimates of throughfall; typical inter-gage spacing for forest studies is on the order of 10 to 30 m (Gash et al. 1980). Large plastic sheets have also been used to get an integrated measure of net rainfall (Calder and Rosier 1976).

Stemflow is measured by attaching flexible troughs tightly around the trunks of trees and conducting the water to rain gages or collecting bottles. Helvey and Patric (1965a) stated that measuring stemflow from all trees on randomly selected plots gives the most representative results, with plot diameters at least 1.5 times the diameter of the crown of the largest trees. However, since stemflow is usually much less than throughfall, most studies have estimated stemflow less rigorously by sampling a few "typical" trees.

The few published studies of grass or litter interception have usually been done using artificial rain, either measuring the net rainfall from small isolated areas in the field (Merriam 1961) or by collecting undisturbed samples of the surface litter and setting them on recording scales in the laboratory (Pitman 1989; Putuhena and Cordery 1996).

7.6.3 Modeling

Modeling via Regression Analysis

Most of the earlier studies of interception have used results of field or laboratory measurements in particular plant communities to establish equations relating Rt, Rs, El, Rn, and/or Ei to R via regression analysis. These equations are usually of the form

$$Y = M_Y \cdot R + B_Y, \qquad \textbf{(7-61)}$$

where Y is one of the components of the interception process (Rt, Rs, Ec, El, or Ei), R is gross rainfall for an individual storm, and M_Y and B_Y are empirical constants determined by regression analysis. Equations in the form of (7-61) can readily be adapted to give estimates for seasonal or annual periods:

$$\Sigma Y = M_Y \cdot \Sigma R + B_Y \cdot n, \qquad \textbf{(7-62)}$$

where the summation sign indicates seasonal or annual totals and n is the number of storms per season or year.

Table 7-7 summarizes published equations for various community types. Unfortunately, few of the studies that developed these equations made concurrent measurements of leaf-area index, so it is difficult to judge the range of applicability of their results.

Only a few studies have included estimates of litter interception loss; most of these have found El in the range $0.02 \cdot R$ to $0.05 \cdot R$, though some higher values have been reported (Helvey and Patric 1965b; Helvey 1971).

As shown in Example 7-7, regression equations can be useful for showing the effects of rainfall amount and number of storms on net rainfall. However, such equations cannot usually be confidently applied to areas other than where they were developed, and they cannot be used to predict the effects of land-cover changes.

EXAMPLE 7-7

Summer gross rainfall at Fairbanks, Alaska, ranges from 100 to 400 mm, typically arriving in about 45 low-intensity storms. Develop relations to estimate the effects of total summer gross rainfall and number of storms on (a) net rainfall and (b) net rainfall as a fraction of gross rainfall in birch forests in this region.

Solution None of the equations listed in Table 7-7 applies to central Alaska, but for purposes of illustration, we use the ones for eastern hardwoods in leaf:

$$\Sigma(Rt + Rs) = 0.941 \cdot \Sigma R - 0.92 \cdot n$$

and assume that $\Sigma El = 0.04 \cdot \Sigma R$. Then, from Equation (7-62), we have

$$\begin{aligned} \Sigma Rn &= 0.941 \cdot \Sigma R - 0.92 \cdot n - 0.04 \cdot \Sigma R \\ &= 0.901 \cdot \Sigma R - 0.92 \cdot n. \end{aligned}$$

Now we can use this relation to estimate ΣRn and $\Sigma Rn/\Sigma R$ for $n = 10$ to 60 storms per season over the range $100 \leq \Sigma R \leq 400$ mm, with the results shown in Figure 7-16.

Conceptual Models

Because of the uncertain transferability of regression equations and the need for simulating interception loss in predictive models, considerable effort has

TABLE 7-7
Regression Equations for Estimating Throughfall, *Rt*, and Stemflow, *Rs*, as Functions of Gross Rainfall, *R*, for Individual Storms. [Equation (7-61)], or for Seasons [Equation (7-62)]

Plant Community	Quantity (Y, cm)	M_Y	B_Y (cm)
Eastern hardwoods full leaf	Rt	0.901	−0.079
	Rs	0.041	−0.013
	$Rt + Rs$	0.941	−0.092
Eastern hardwoods leafless	Rt	0.914	−0.038
	Rs	0.062	−0.013
	$Rt + Rs$	0.978	−0.051
Red pine	$Rt + Rs$	0.89	−0.10
Loblolly pine	$Rt + Rs$	0.88	−0.08
Shortleaf pine	$Rt + Rs$	0.91	−0.10
Eastern white pine	$Rt + Rs$	0.91	−0.13
Ponderosa pine	$Rt + Rs$	0.93	−0.15
Pines (average)	$Rt + Rs$	0.90	−0.10
Spruce-fir-hemlock	$Rt + Rs$	0.79	−0.13

Eastern hardwood values from Helvey and Patric (1965b), conifer values from Helvey (1971).

FIGURE 7-16

(a) Net rainfall, *Rn*, and (b) the ratio of net rainfall to gross rainfall, *Rn*/*R*, as a function of seasonal gross rainfall, *R*, and number of storms per season, *n*, estimated for a central Alaskan birch forest.

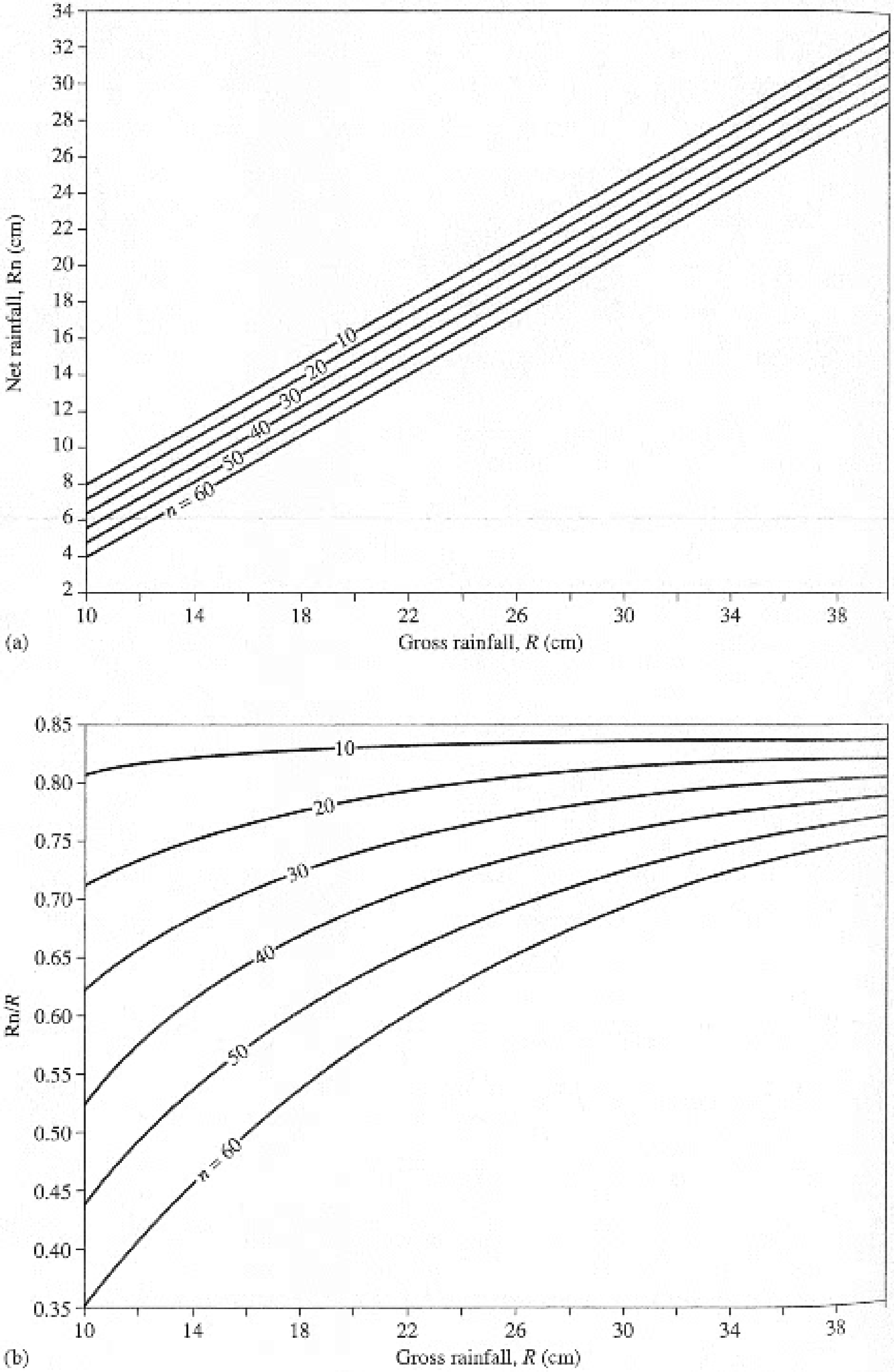

been expended to develop conceptual models of the process. The most widely used of these was originally developed by Rutter et al. (1971) and modified by Gash and Morton (1978) and Valente et al. (1997). In this model the area of interest is partitioned into the fraction covered by a forest canopy (F) and the open fraction $(1 - F)$. The model computes a running water balance of the canopy (leaves and branches) and the tree trunks using the conceptual scheme shown in Figure 7-17 and a time step (Δt) of 1 day.

The canopy storage is filled by rainfall and emptied by drainage and evaporation. Drainage from the

FIGURE 7-17
The "sparse" Rutter conceptual model of interception as developed by Valente et al. (1997). See text for explanation.

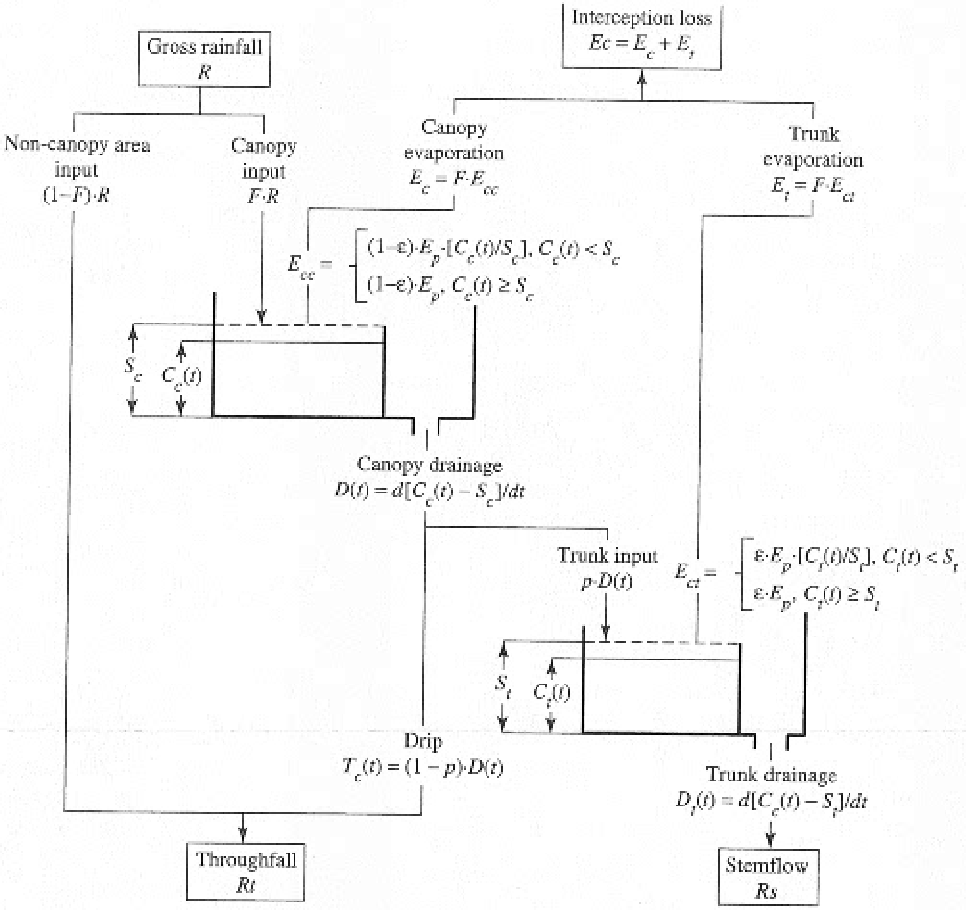

canopy occurs when the canopy storage capacity S_c is exceeded. A small fraction p of this drainage becomes stemflow. Throughfall (*Rt* in Figure 7-15) is the sum of the rain falling in open areas plus the fraction of drainage that drips from the canopy $(1 - p)$. When the actual amount of water on the canopy, $C_c(t)$, exceeds S_c, evaporation from the canopy, $E_c(t)$, occurs at the rate given by the Penman Equation [Equation (7-55)]; when $C_c(t) < S_c$ the evaporation rate equals the Penman rate times $(1 - \varepsilon)\cdot C_c(t)/S_c$, where ε is the fraction of total evaporation that occurs from the trunks. The interception loss from the canopy-covered area is the sum of the evaporation from trunks and canopy. The canopy interception loss for the entire area (*Ec* in Figure 7-15) is the sum of the evaporation from the canopy and the trunks multiplied by the canopy-covered fraction, F.

The structure of the vegetation is reflected in the parameters S_c, S_t, p, and ε. Valente et al. (1997) discuss how these can be determined from analysis of regression relations of the form of Equation (7-61) developed from field measurements. Typical values of S_c are in the range 0.2–1.1 mm. The quantities involved in stemflow and evaporation from trunks are small: the few measured values suggest $S_t < 0.02$ mm, $p < 0.03$ and $\varepsilon \approx 0.023$.

Several studies have found good agreement between observed interception loss and that simulated by the Rutter model and its variants (e.g., Gash and Morton 1978; Gash 1979; Lloyd et al. 1988; Valente 1997). However, such models clearly require extensive field studies to establish the canopy-structure parameters. The computation of interception in the BROOK90 model uses a simplified version of the Rutter model, as described in Box 7-2.

The Penman Equation is appropriate for computing the rate of evaporation of intercepted water because the evaporation is from the leaf surface and stomata are not involved (this is equivalent to an infinite canopy conductance in the Penman–Monteith Equation). Thus canopy evaporation rates

BOX 7-2

Computation of Interception in the BROOK90 Model

The capacity of the vegetation to store intercepted rain, *INTRMX*, is related to the leaf-area index, *LAI*, and the analogously defined stem-area index, *SAI*, by the formula

$$INTRMX = CINTRL \cdot LAI + CINTRS \cdot SAI, \qquad \textbf{(7B2-1)}$$

where the default values are $CINTRL = CINTRS = 0.15$ mm. These values give $INTRMX = 1.0$ mm at typical forest values of $LAI = 6$ and $SAI = 0.7$. Prior to filling the canopy capacity, the rate of canopy interception, *RINT*, is computed as a fraction of the rainfall rate, *RFAL*; that is,

$$RINT = (FRINTL \cdot LAI + FRINTS \cdot SAI) \cdot RFAL, \qquad \textbf{(7B2-2)}$$

where the default values are $FRINTL = FRINTS = 0.06$. With these values and the typical *LAI* and *SAI* values, $RINT = 0.40 \cdot RFAL$.

The rate of evaporation of intercepted water is calculated from the Penman–Monteith Equation [Equation (7-56)] with infinite canopy conductance, as in Example 7-8. The storage of water on the canopy is tracked using standard water-balance accounting, as in the Rutter model (Figure 7-17).

will be larger than transpiration rates for the same conditions. For forests, the difference is considerable because of the effects of roughness on the efficiency of turbulent transfer, as illustrated by Example 7-8.

EXAMPLE 7-8

Compare the canopy evaporation rate with the transpiration rates for the pine forest at Thetford, England, for the conditions of Example 7-6.

Solution The atmospheric conductance for Example 7-6 is 0.232 m s^{-1}. Substituting that and the other appropriate values into Equation (7-55) yields a canopy evaporation rate of 6.21×10^{-4} mm s^{-1} or 53.6 mm day^{-1}, over 40 times greater than the transpiration rate with $\Delta\theta = 0$ cm. Thus if there is 1 mm of intercepted water on the canopy, this water will be completely evaporated in (1 mm)/(6.21×10^{-4} mm s^{-1}) = 1610 s = 0.45 hr.

It is of interest to compare the latent-heat flux, *LE*, associated with the evaporation of this intercepted water with the available energy (net radiation). This flux is calculated as

$$\begin{aligned} LE &= \rho_w \cdot \lambda_v \cdot E = (1000 \text{ kg m}^{-3}) \cdot (2.45 \text{ MJ kg}^{-1}) \\ &\quad \cdot (6.21 \times 10^{-7} \text{ m s}^{-1}) \\ &= 0.00152 \text{ MJ m}^{-2} \text{ s}^{-1}, \end{aligned}$$

which is about 8.4 times the net radiation. The difference between the latent-heat flux and the net radiation must be supplied by downward sensible-heat transfer from air-advected energy. Several studies have shown that such advection is commonly involved in evaporating intercepted water (e.g., Stewart 1977)—that is, interception loss can markedly cool the air.

The contrast between rates of evaporation of intercepted water and rates of transpiration illustrated in Example 7-8 have important bearing on understanding the hydrologic impacts of land-use changes, as discussed in Section 7.6.4.

7.6.4 Hydrologic Importance of Interception Loss

As shown in Table 7-8, interception loss ranges from 10 to 40% of gross precipitation in various plant communities. There has been considerable debate concerning the extent to which this loss is an addition to, as opposed to a replacement for, water loss by transpiration.

Clearly most of the interception loss that occurs in seasons when vegetation is dormant is a net addition to evapotranspiration. When intercepted water is present during the growing season, it evaporates in preference to water in stomatal cavities because it does not encounter stomatal resistance. However, in forests the evaporation of intercepted water occurs at rates several times greater than for transpiration under identical conditions. (See Example 7-8.) Thus intercepted water disappears quickly and interception loss replaces transpiration only for short periods. For example, Stewart (1977) found that annual interception loss for the forest he studied was 214 mm, and that 69 mm would have transpired during the time this loss was occurring. Thus the net additional evapotranspiration due to interception was 145 mm; this was 26% of the total annual evapotranspiration.

For short vegetation, atmospheric conductances are much lower than over forests (Figure